

# Engineering Notes

## Efficient Initial Costates Estimation for Optimal Spiral Orbit Transfer Trajectories Design

Donghun Lee\* and Hyochoong Bang†

*Korea Advanced Institute of Science and Technology,  
 Daejeon, 305-701, Republic of Korea*

DOI: 10.2514/1.44550

### Introduction

A N INITIAL costates estimation method to solve optimal transfer orbit design problems is presented here. The target orbits are spiral trajectories with low-thrust input. Fuel optimal trajectory design problems have been previously investigated for a number of orbit transfer applications and interplanetary missions [1–7]. Among representative techniques is an indirect approach based on the variational principle, through which the optimal control problems can be converted into a two-point boundary value problem. Transfer orbit design problems can be solved by finding the unknown initial costate variables, but the indirect method suffers from some critical drawbacks, such as a small radius of convergence. The estimation of initial costates for spiral trajectory design is particularly difficult due to a long transfer time and the multirevolution nature of such trajectories. Several advanced indirect methodologies, including functional approximation, continuation, homotopy, and the step-by-step approach, have been adopted to compute initial unknown costates [1,2,8,9].

In [1], properties of the initial costates were exploited to estimate the initial costates. In that work, the terminal specific energy with respect to the Earth and the initial radius of the circular orbit were fixed. The initial costates of the radial distance and tangent velocity can be approximated using exponential functions versus time; however, the initial costate behaviors of radial velocity were not fully analyzed in [1]. Furthermore, if the initial radius, terminal specific energy, and central planet are changed, additional steps, such as determining a new curve fitting, may be necessary to design optimal trajectories with a longer transfer time.

In this study, a new initial guess structure for costates is proposed to construct optimal spiral trajectories using the arbitrary initial radius, transfer time, terminal target energy, and central planet. The proposed initial guess structure requires neither functional approximation nor extrapolation. The structure is developed according to initial costate properties, and it can accommodate specific energy targeting problems.

### Problem Definition

In this section, a specific energy targeting problem is investigated. The same system state dynamics are presented in [1,2].

Received 24 March 2009; revision received 23 June 2009; accepted for publication 23 June 2009. Copyright © 2009 by the American Institute of Aeronautics and Astronautics, Inc. All rights reserved. Copies of this paper may be made for personal or internal use, on condition that the copier pay the \$10.00 per-copy fee to the Copyright Clearance Center, Inc., 222 Rosewood Drive, Danvers, MA 01923; include the code 0731-5090/09 and \$10.00 in correspondence with the CCC.

\*Ph.D. Candidate, Division of Aerospace Engineering, 335 Gwahangno, Yuseong.

†Professor, Division of Aerospace Engineering, 335 Gwahangno, Yuseong. Senior Member AIAA.

$$\dot{r} = v_r \quad (1)$$

$$\dot{v}_r = (v_\theta^2/r) - (\mu/r^2) + a_{\text{ref}}u \sin(\alpha) \quad (2)$$

$$\dot{v}_\theta = -(v_\theta v_r/r) + a_{\text{ref}}u \cos(\alpha) \quad (3)$$

$$\dot{\theta} = (v_\theta/r) \quad (4)$$

where  $a_{\text{ref}}$  represents a reference acceleration magnitude, and  $u$  and  $\alpha$  are command inputs, with  $u$  a normalized acceleration magnitude and  $\alpha$  an in-plane thrust angle. The low thrust is assumed to be an unconstrained variable specific impulse (VSI) type of engine, for which the thrust magnitude is modulated by the specific impulse. The mass flow dynamics are prescribed as

$$\dot{m} = -\frac{T}{v_e} = -\frac{2\varepsilon P}{I_{\text{sp}}^2 g_0^2} \quad (5)$$

where  $I_{\text{sp}}$  denotes specific impulse,  $g_0$  is the Earth's gravitational acceleration at sea level,  $P$  is engine power, and  $\varepsilon$  is engine efficiency. To minimize fuel consumption for an unconstrained VSI engine with a fixed transfer time, the spacecraft mass and power are decoupled from the problem, and only the accumulated thrust acceleration affects the spacecraft propellant [1].

$$\frac{1}{m_f} - \frac{1}{m_0} = \frac{1}{2} \int_{t_0}^{t_f} \frac{a^2}{P} dt = \frac{a_{\text{ref}}}{2P} \int_{t_0}^{t_f} u^2 dt \quad (6)$$

In Eq. (6), the denominator  $P$  is constant at all times, and the numerator term,  $a_{\text{ref}}$ , to be determined later, is also constant. Therefore, the denominator  $P$  and the numerator term,  $a_{\text{ref}}$ , do not affect the optimal cost. Finally, the cost is adjusted as a square of the normalized thrust magnitude to minimize fuel consumption, such that

$$J = v(\varepsilon - \varepsilon_t) - \int_{t_0}^{t_f} u^2 dt \quad (7)$$

where  $\varepsilon (=v^2/2 - \mu/r)$ , and  $\varepsilon_t$  corresponds to the specific target energy of the spacecraft with respect to the central body.

The Hamiltonian, optimality, necessary, and boundary conditions can be derived from the variational principle. By applying typical optimal control formulation, the following set of equations can be readily derived [1,2]:

$$\dot{\lambda}_r = -\frac{\partial H}{\partial r} = \lambda_{vr} \left( \frac{v_\theta^2}{r^2} - \frac{2\mu}{r^3} \right) - \lambda_{v\theta} \left( \frac{v_r v_\theta}{r^2} \right) + \lambda_\theta \left( \frac{v_\theta}{r^2} \right) \quad (8)$$

$$\dot{\lambda}_{vr} = -\frac{\partial H}{\partial v_r} = -\lambda_r + \lambda_{v\theta} \left( \frac{v_\theta}{r} \right) \quad (9)$$

$$\dot{\lambda}_{v\theta} = -\frac{\partial H}{\partial v_\theta} = -2\lambda_{vr} \left( \frac{v_\theta}{r} \right) + \lambda_{v\theta} \left( \frac{v_r}{r} \right) - \lambda_\theta \left( \frac{1}{r} \right) \quad (10)$$

$$\dot{\lambda}_\theta = -\frac{\partial H}{\partial \theta} = 0 \quad (11)$$

The optimal control input can be derived such that

$$\alpha = \tan^{-1}(\lambda_{vr}/\lambda_{v\theta}) \quad (12)$$

$$u = \frac{\lambda_{vr} a_{ref} \sin(\alpha) + \lambda_{v\theta} a_{ref} \cos(\alpha)}{2} \quad (13)$$

Therefore, the actual acceleration is calculated as

$$a_{vr} = a_{ref} u \sin(\alpha) = (a_{ref}^2/2) \lambda_{vr} \quad (14)$$

$$a_{v\theta} = a_{ref} u \cos(\alpha) = (a_{ref}^2/2) \lambda_{v\theta} \quad (15)$$

and the boundary conditions for costate variables satisfy

$$\lambda_r(t_f) = v(\mu/r^2) \quad (16)$$

$$\lambda_{vr}(t_f) = v(v_r) \quad (17)$$

$$\lambda_{v\theta}(t_f) = v(v_\theta) \quad (18)$$

$$\lambda_\theta(t_f) = 0 \quad (19)$$

The unknown parameters are the three initial costates of  $\lambda_r$ ,  $\lambda_{vr}$ , and  $\lambda_{v\theta}$  and one multiplier,  $v$ , which is associated with the targeted condition. And the terminal boundary conditions consist of three final costate variables and the target-specific energy.

### Initial Costate Behaviors and New Initial Guess Structure

In this section, the initial costate behaviors are analyzed, and a method to guess the unknown initial costates for the specific energy targeting problem is proposed. A generalized approach can be applied to handle any initial radius of circular orbit, terminal specific energy, central planet, and long transfer time without interpolation. For this goal, several Earth escape trajectories were constructed using the discrete continuation method to analyze the initial costate behaviors [3].

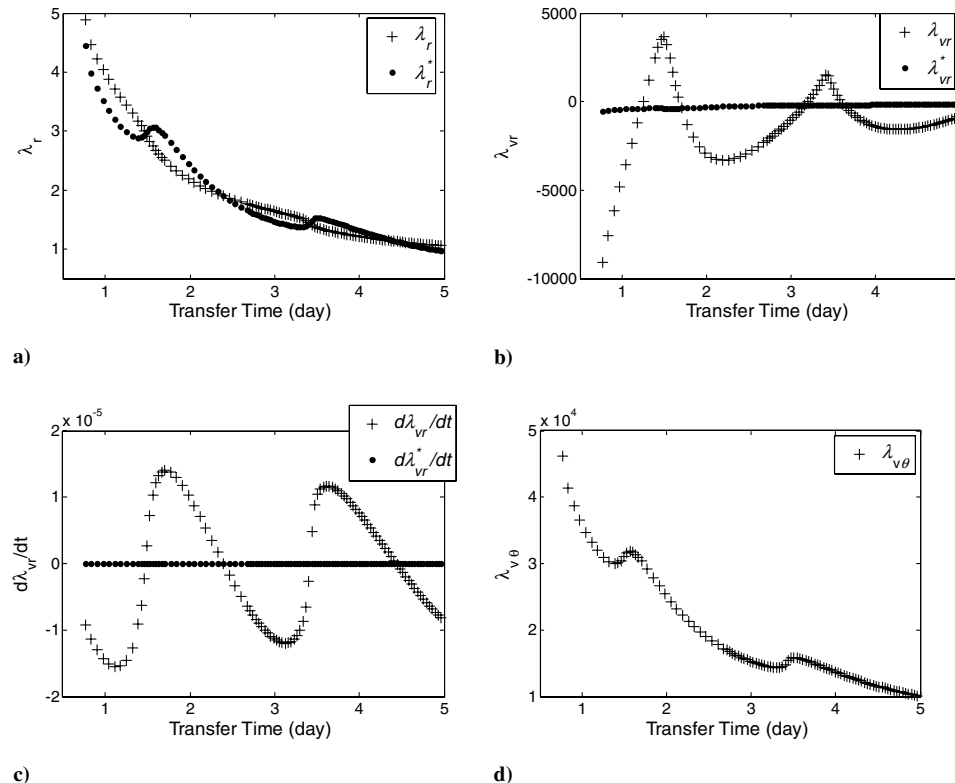


Fig. 1 Transfer time versus initial costate history and estimated initial costate using true  $\lambda_{v\theta}$ : a)  $\lambda_r$ , b)  $\lambda_{vr}$ , c)  $\dot{\lambda}_r$ , d)  $\lambda_{v\theta}$ . Solution: cross, estimated value: dots.

First, minimum-propellant Earth escape trajectories are solved while initial states are fixed for a high-altitude circular orbit with an initial radius of, for example, 35,000 km, and the transfer time is gradually increased from 66,000 s to 5 days. As seen in Fig. 1, the initial costates of  $\lambda_r$  and  $\lambda_{vr}$  exponentially decrease as the transfer time increases, and similar results were observed in [1,3]. Optimal initial  $\lambda_{v\theta}$  also tends to decrease with oscillatory behavior, which was not addressed in [1].

Next, a similar approach is applied for the initial radius of a circular orbit with a fixed transfer time. The conditions from a circular orbit with a 35,000 km radius gradually decrease to a circular orbit with a 7000 km radius. The initial costate histories exhibit discontinuity trends for  $\lambda_{vr}$ , as shown in Fig. 2.

The minimum value of  $\lambda_{vr}$  increases as the initial radius increases. For the initial costates of  $\lambda_r$  and  $\lambda_{v\theta}$ , a similar property appears, as in Fig. 1. The properties observed so far can be summarized as 1) the initial  $\lambda_r$  and  $\lambda_{v\theta}$  decrease as the transfer time and initial radius increase; 2) the initial  $\lambda_{vr}$  oscillates about zero whereas the transfer time and initial radius vary; 3) in Figs. 1 and 2, the estimated  $\lambda_r$  was calculated with the given  $r$ ,  $v_r$ , and true  $\lambda_{v\theta}$  by the following relation as Eq. (20). We can see that there exists a linear property between the initial  $\lambda_r$  and  $\lambda_{v\theta}$ :

$$\lambda_r \approx \lambda_{v\theta}(v_\theta/r) \quad (20)$$

and 4) in the history of  $\dot{\lambda}_r$  from Fig. 2, several points appear to be discontinuous. Between the discontinuous points, optimal trajectories are formed by the same number of revolutions. When  $r(0)$  lies between 22,000 and 26,000 km, the optimal trajectories exhibit the same number of revolutions, such as 5. When  $r(0)$  is between 19,000 and 22,000 km, the number of revolutions is 6, and the number of revolutions increases as the initial radius decreases.

Motivated by those properties, a new initial guess structure is proposed for the arbitrary target-specific energy, central planet, initial orbit radius (circular orbit), and any transfer time as follows:

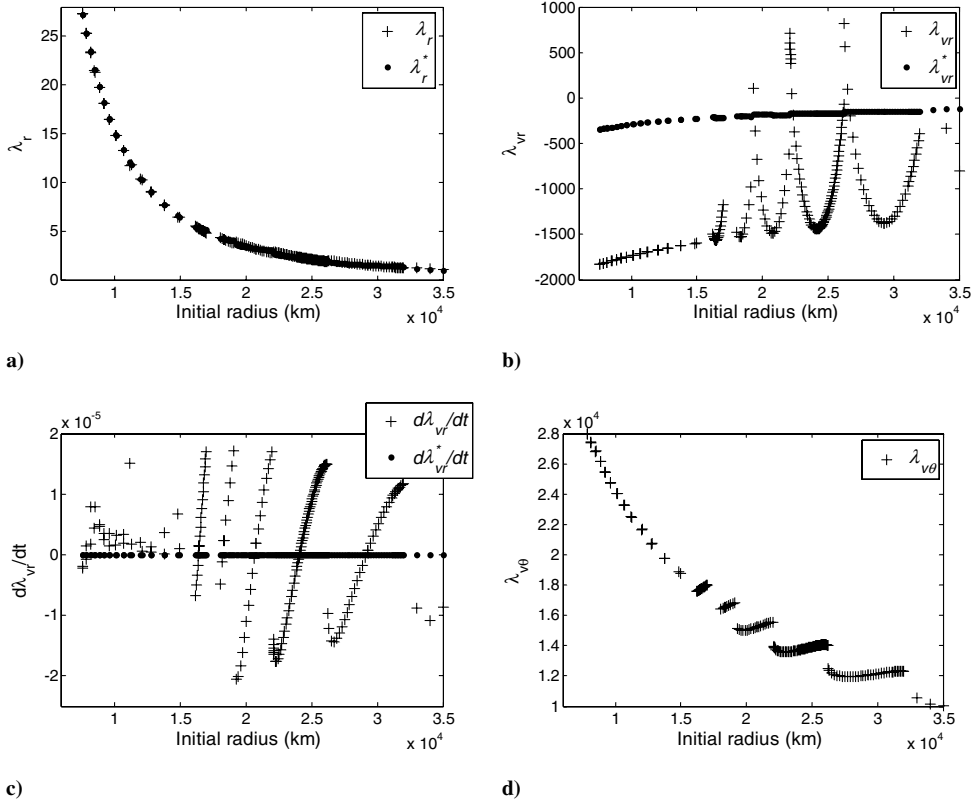


Fig. 2 Initial radius versus initial costate history and estimated initial costates using true  $\lambda_{v\theta}$ : a)  $\lambda_r$ , b)  $\lambda_{vr}$ , c)  $\dot{\lambda}_r$ , and d)  $\lambda_{v\theta}$ . Solution: cross, estimated value: dots.

$$\lambda_{\text{guess}} = \begin{bmatrix} \lambda_r(t_0) \\ \lambda_{vr}(t_0) \\ \lambda_{v\theta}(t_0) \end{bmatrix} = \begin{bmatrix} \kappa(v_\theta(t_0)/r(t_0)) \\ -0.012\kappa \\ \kappa \end{bmatrix} \quad (21)$$

where  $v_\theta(t_0)$  and  $r(t_0)$  are the given initial tangential velocity and initial radius.

$\dot{\lambda}_{vr}(t_0)$  was set to 0, because  $\dot{\lambda}_{vr}(t_0)$ , which is an initial time derivative of  $\lambda_{vr}$ , is oscillating across the zero-crossing line, as in Figs. 1 and 2. Using this behavior of  $\dot{\lambda}_{vr}(t_0)$ ,  $\lambda_r$  can be evaluated from  $\lambda_{v\theta}$  with the following costate dynamics equation:

$$\dot{\lambda}_{vr} = -\lambda_r + \lambda_{v\theta}(v_\theta/r) \quad (22)$$

From Eq. (22), by setting  $\dot{\lambda}_{vr}$  to 0, a linear property between  $\lambda_r$  and  $\lambda_{v\theta}$  can be established, as in Eq. (21). In Eq. (21),  $\lambda_r$  decreases as the initial radius increases.

In this structure,  $\lambda_{vr}$  is assigned a negative value of near zero for the following reasons: 1) as in Figs. 1 and 2,  $\lambda_{vr}$  tends to oscillate near the zero-crossing line, but the middle value is not 0; and 2) whenever  $\dot{\lambda}_{vr}(t_0)$  is 0,  $\lambda_{vr}$  is not 0. Therefore, a negative ratio is selected as  $-0.012$  between  $\lambda_{vr}$  and  $\lambda_{v\theta}$ ; this is indicated with a dot in Fig. 1. The resultant initial steering angle is  $-0.6$  deg, which is close to 0. The effective steering direction is nearly aligned with the velocity direction [10]. In this note, the initial orbit is circular; therefore, the steering direction is almost 0, but is not always 0, as it is in [1–3].

In Eq. (21), the only unknown parameter is  $\kappa$ , which is equal to  $\lambda_{v\theta}$ . When the transfer time decreases, more acceleration is required for orbit transfer; therefore,  $\lambda_{v\theta}$  should become larger in Eq. (15). The reverse is true for an increase in transfer time. The parameter  $\kappa$  is determined by numerical integration with the initial costate structure and system dynamics. The unknown value of multiplier  $v$ , which is associated with the target condition, was chosen from Eq. (16), such that

$$v = \frac{\lambda_r r^2}{\mu} \Big|_{t=t_f} \quad (23)$$

The method to determine  $\kappa$  is addressed in the next section with numerical examples. For the previous initial guess problem, it was necessary to guess the four variables of  $\lambda_r$ ,  $\lambda_{vr}$ ,  $\lambda_{v\theta}$ , and  $v$ ; in the new structure, only the single parameter  $\kappa$  needs to be initialized, which is sufficient for the initial estimation of all costates.

## Numerical Examples

Choosing a proper  $\kappa$  value and selecting a specific interval for  $\kappa$  are not difficult. In fact,  $\kappa$  is chosen by inspection with numerical integration. Many approaches could be considered to find the desirable interval and tune  $\kappa$ . We explain an easy way to locate a good interval with case 1 under the conditions given in Table 1. First, with a large interval and a large increment, the system dynamics and the costate dynamics are numerically integrated, and the terminal constraints of the specific energy are evaluated.

At first, the interval of  $\kappa$  lies between 10,000 and 250,000, and the increment is 10,000. There exists a zero-crossing line for  $\kappa$  between 190,000 and 200,000. Thus, it can be claimed that there is a proper value for  $\kappa$  between 190,000 and 200,000, so that the interval of  $\kappa$  is modified between 190,000 and 200,000, and the increment of  $\kappa$  is modified into a smaller value such as 1000. After evaluating the terminal constraint of specific energy, we can modify the interval of  $\kappa$  between 199,000 and 200,000, and the increment of  $\kappa$  is modified into 100. By taking such sequences, we could find desirable intervals. And when  $\kappa$  is 199,300, the terminal specific energy is close to the target-specific energy. Thus, for the good initial guess structure,  $\kappa$  is finally selected as 199,300. This approach is quite simple and enables us to find an effective interval. By this approach, we were able to specify a proper value for  $\kappa$  for all of the problems in this study.

Eight examples are presented in Table 1, for which the initial radius, central body, specific target energy, or transfer time are different from the previous conditions. Using the initial guess structure

Table 1 Conditions and the solutions of the numerical examples

Case No.	$t_f$ , days	$r_0$ , km	$\varepsilon_t$ , km <sup>2</sup> /s <sup>2</sup>	Central body	$a_{ref}$ , km/s <sup>2</sup>	$\kappa$	$\lambda_r$ : solution (guess)	$\lambda_{v\theta}$ : solution (guess)
1	41	7000	-1.7	Earth	$4 \times 10^{-6}$	199,300	216.39 (214.85)	199,092.20 (199,300)
2	200	6693	-2.4	Earth	$1 \times 10^{-6}$	639,300	737.23 (737.13)	639,969.4 (639300)
3	300	6673	0.0	Earth	$5 \times 10^{-7}$	2,188,300	2534.08 (2534.51)	2,179,550.1 (2,188,300)
4	150	6673	-0.7	Earth	$1 \times 10^{-6}$	1,007,700	1165.59 (1167.13)	996,935.7 (1,007,700)
5	20	1838	0.0	Moon	$1 \times 10^{-6}$	-1,420,000	-1161.38 (-1152.90)	-1,414,989.9 (-1,420,000)
6	40	1838	-0.2	Moon	$5 \times 10^{-7}$	-1,980,000	-1615.75 (-1607.53)	-1,989,274.4 (-1,980,000)
7	150	7594	0.0	Earth	$1 \times 10^{-6}$	1,098,800	1,272.90 (1,272.64)	1,100,493.6 (1,098,800)
8	120	6693	GEO	Earth	$1 \times 10^{-6}$	893,000	1,040.53 (1,040.36)	898,042.80 (893,000)

with the appropriate  $\kappa$  and shooting algorithm, optimal spiral trajectories can be effectively generated with just a few iterations, as shown in Table 1. Figure 3 presents results of the six optimal spiral trajectories. The first four plots display optimal trajectories with the Earth as a central body. The remaining plots show optimal moon capture trajectories with the system dynamics integrated backward, so that the signs of  $\lambda_r$  and  $\lambda_{v\theta}$  are negative. One of the significant results is that the errors between the solutions and guesses for  $\lambda_r$  and  $\lambda_{v\theta}$  are less than 1%. All the cases were solved by using the new initial guess structure with only a few iterations. This illustrates the effectiveness of the new initial guess structure approach proposed in this study.

The specific energy targeting problem with a constraint on thruster magnitude with a VSI-type engine can be solved by the initial guess structure as proposed in this Note. In the example of case 7, the initial orbit is a circular orbit with a radius of 7594 km and a 150 day transfer time with the target-specific energy equal to 0. We assume that the normalized thrust magnitude controlled by  $I_{sp}$  is constrained between 0.52 and 0.58. In Eq. (21),  $\kappa$  is selected as 1,098,800, and the problem is solved with the initial costate structure approach. As a result, the initial guess set of costates are quite close to the solution.

Case 8 is a minimum-propellant problem, for which the terminal constraint is a specific target set. In case 8, the initial orbit is a 6693 km circular orbit, whereas the terminal orbit is a 42,241 km circular orbit with the given transfer time of 150 days. Using  $\kappa$  equal to 898,300 and the initial guess structure technique, we were able to find the optimal trajectory. Also, some orbit raising problems such as case 8 with terminal constraints in terms of specific target set can be solved using the proposed initial guess structure.

Using the given initial guess set in Eq. (21), all problems cannot be solved. This is because the given initial guess structure is derived primarily for a specific energy targeting problem with an initial circular orbit. In previous papers, the specific energy targeting

problem for low thrust has been investigated for initial circular orbits [1–7,9]. Thus, we focused on the initial circular orbit for a similar type of problem. A modified initial guess structure may be needed to solve another set of problems for an initial elliptic orbit and other specific terminal constraint sets. One important point in the paper is that some costate properties exist for the set of the problems concerning transfer time and initial conditions. Such properties make long transfer time problems easy to solve using the initial guess structure strategy.

Also, in this Note, the proposed initial guess structure is developed using a VSI-type engine system. Thus, applying the initial guess structure to the constant specific impulse (CSI) type of engine for which optimal control is determined by switching function may not be appropriate. After the trend of the initial costate is examined with a CSI-type engine, a proper initial guess structure may be developed. An alternative way to apply the given initial set in Eq. (21) to the CSI-type engine is to adopt the algorithm addressed in [9].

## Conclusions

Initial costate behaviors over the transfer time and initial radius of a circular orbit were examined here for the minimum-fuel, planar, and specific energy targeting problems. The costates of radial distance and of tangential velocity exponentially decrease as the transfer time or initial radius increases. The costates of the radial velocity are oscillatory, whereas the transfer time or initial radii are varied. Based on the initial costate properties, a new initial guess structure was proposed to solve the indirect optimization problem. In the proposed method, only the parameter  $\kappa$  is needed to set the structure of the initial guess. Through several examples, it was demonstrated that this method is able to efficiently produce solutions for designing optimal spiral trajectories for the arbitrary central planet, long transfer time, initial radius, and terminal target-specific energy conditions.

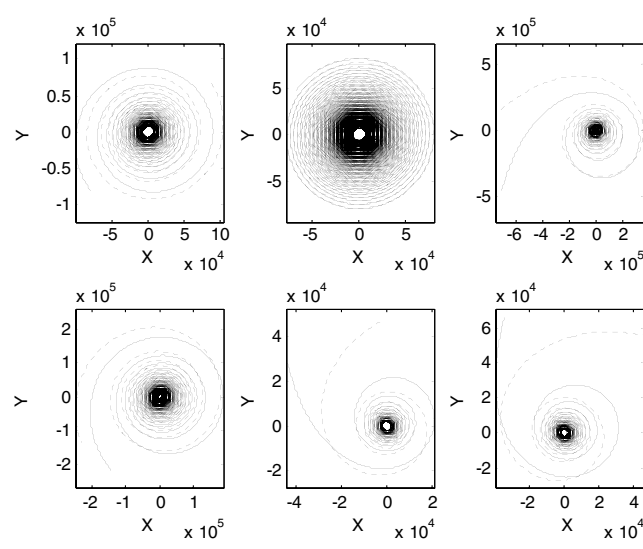
## Acknowledgment

This research was supported by National Space Lab program through the Korea Science and Engineering Foundation funded by the Ministry of Education, Science and Technology (S10801000123-08A0100-12310).

## References

- [1] Ranieri, C. L., and Ocampo, C. A., "Indirect Optimization of Spiral Trajectories," *Journal of Guidance, Control, and Dynamics*, Vol. 29, No. 6, 2006, pp. 1360–1366.  
doi:10.2514/1.19539
- [2] Pierson, B. L., and Kluever, C. A., "Three-Stage Approach to Optimal Low-Thrust Earth-Moon Trajectories," *Journal of Guidance, Control, and Dynamics*, Vol. 17, No. 6, 1994, pp. 1275–1282.  
doi:10.2514/3.21344
- [3] Lee, D., and Bang, H. C., "Optimal Earth escape trajectories using Discrete Continuation and Costate Estimator," AAS Paper 08-197 2008.
- [4] Ranieri, C. L., and Ocampo, C. A., "Indirect Optimization of Three-Dimensional Finite-Burning Interplanetary Transfers Including Spiral Dynamics," *Journal of Guidance, Control, and Dynamics*, Vol. 32, No. 2, 2009, pp. 444–454.  
doi:10.2514/1.38170
- [5] Ranieri, C. L., and Ocampo, C. A., "Indirect Optimization of Two-Dimensional Finite-Burning Interplanetary Transfers Including Spiral

Fig. 3 The guessed trajectories (dotted line) and the optimal trajectories (solid line) using initial guess structure (from the upper left: Cases 1–3, from the bottom left: Cases 4–6).



Dynamics," *Journal of Guidance, Control, and Dynamics*, Vol. 31, No. 3, 2008, pp. 720–728.  
doi:10.2514/1.30833

[6] Vadali, S. R., Nah, R., Braden, E., and Johnson, I. L., Jr., "Fuel-Optimal Planar Earth-Mars Trajectories Using Low-Thrust Exhaust-Modulated Propulsion," *Journal of Guidance, Control, and Dynamics*, Vol. 23, No. 3, 2000, pp. 476–482.  
doi:10.2514/2.4553

[7] Nah, R., Vadali, S. R., and Braden, E., "Fuel-Optimal, Low-Thrust, Three-Dimensional Earth–Mars Trajectories," *Journal of Guidance, Control, and Dynamics*, Vol. 24, No. 6, 2001, pp. 1100–1107.  
doi:10.2514/2.4844

[8] Thorne, J. D., and Hall, C. D., "Approximate Initial Lagrange Costates for Continuous-Thrust Spacecraft," *Journal of Guidance, Control, and Dynamics*, Vol. 19, No. 2, 1996, pp. 283–288.  
doi:10.2514/3.21616

[9] Haberkorn, T., Martinon, P., and Gergaud, "Low-Thrust Minimum-Fuel Orbital Transfer: A Homotopic Approach," *Journal of Guidance, Control, and Dynamics*, Vol. 27, No. 6, 2004, pp. 1046–1060.  
doi:10.2514/1.4022

[10] Kluever, C. A., "Simple Guidance Scheme for Low-Thrust Orbit Transfers," *Journal of Guidance, Control, and Dynamics*, Vol. 21, No. 6, 1998, pp. 1015–1017.  
doi:10.2514/2.4344